

# Raman scattering test of single-wall carbon nanotube composites

V. G. Hadjiev<sup>a)</sup>

*Institute for Space Systems Operations and Texas Center for Superconductivity, University of Houston, Houston, Texas 77204-5932*

M. N. Iliev

*Texas Center for Superconductivity, University of Houston, Houston, Texas 77204-5932*

S. Arepalli and P. Nikolaev

*G. B. Tech./Lockheed Martin, 2400 NASA Road One, Mail Stop C61, Houston, Texas 77058*

B. S. Files

*NASA Johnson Space Center, Houston, Texas 77058-3696*

(Received 17 August 2000; accepted for publication 27 March 2001)

Raman spectroscopy is used to infer elastic properties of single-wall carbon nanotubes (SWNTs) in composites. This letter presents strain-induced frequency shift of tangential Raman active modes of SWNTs embedded in epoxy resin subjected to bending. Epoxy curing and sample extension in the tensile strength test are found to create residual strains on the SWNT ropes. We demonstrate that specimen compression in combination with the Raman microprobe technique provides a means for determining of these strains and hence load transfer effectiveness. © 2001 American Institute of Physics. [DOI: 10.1063/1.1373405]

Single-wall nanotubes (SWNTs) are believed to be the ultimate reinforcement material in polymer composites, due to their high aspect ratio (up to  $10^4$ ), Young's modulus ( $\sim 10^3$  GPa) close to that of diamond,<sup>1</sup> tensile strength of  $\sim 50$  GPa,<sup>2</sup> and light weight (density of  $\sim 1.3$  g/cm<sup>3</sup>).<sup>3</sup> In practice, preparation of high strength nanocomposites has yet to overcome several obstacles. SWNTs form different diameter crystalline nanoropes that usually exhibit bends and loops.<sup>1</sup> As the rope diameter increases, shear deformation reduces the effective moduli of nanoropes by an order of magnitude with respect to that of a SWNT.<sup>4</sup> Therefore, controllable dispersion and alignment of SWNTs in composites are desirable to achieve improvement of the mechanical properties. In addition, interface region properties are known to be crucial for load sharing between the matrix and the reinforcement material.<sup>5</sup> There is little knowledge of the interface region in nanocomposites since direct studies<sup>2,4</sup> are obstructed by the nanosize diameter and high aspect ratio of a SWNT/rope.

In this letter, we report an application of Raman spectroscopy for nondestructive studies of residual strains and load transfer in nanocomposites. The few reports<sup>6</sup> on the application of Raman spectroscopy to nanocomposites have dealt with the second order  $D^*$  band at  $\sim 2650$  cm<sup>-1</sup>. However, this Raman band is rather complicated to interpret because of the modes dispersion involved in the scattering process.<sup>1</sup> Instead, we focus our study on the graphite-like carbon vibrations at  $\sim 1590$  cm<sup>-1</sup>. These modes have been studied in detail by several theoretical approaches.<sup>1</sup>

SWNTs produced by laser ablation<sup>7</sup> were purified and dispersed in Shell epon resin 862/EPI-CURE W<sup>8</sup> at 1 wt % loading. The epoxy-nanotube mixture was cured at 170 °C and a bar ( $2 \times 5 \times 50$  mm) was prepared and cut into two

specimens. The first specimen (a small piece of material) was measured as prepared ("unstressed" specimen A). Elastic properties of the second specimen were first determined by a standard tensile strength test to failure ("stressed" specimen B). For subsequent Raman measurements the B specimen was loaded in a four-point bending rig in compression to a maximum surface strain  $\epsilon_s$  of  $-0.45\%$ . Surface strain was measured by means of a 120  $\Omega$  resistance gage. Our estimates<sup>9</sup> show that the top layer of the composite has experienced uniform compression. Raman spectra, excited with Ar<sup>+</sup> (514.5 nm) and HeNe (632.8 nm) laser lines, were recorded on a multichannel spectrometer in a backward scattering configuration with parallel incident and scattered light polarizations. The laser power density was kept less than 500 W/cm<sup>2</sup>. The spectrometer slits were set to 2.5 cm<sup>-1</sup> spectral width and absolute accuracy of 0.5 cm<sup>-1</sup>. The exciting laser spot of diameter  $\approx 2$   $\mu$ m was kept at one and the same position, close to the strain gauge, throughout the experiment. A reference epoxy-resin sample has given structureless Raman response under 514.5 nm excitation.

Figure 1 shows the low-frequency part of the Raman spectra with bands corresponding to the radial breathing type vibrations (RB modes,  $A_{1(g)}$  symmetry). Within experimental accuracy, the position of the strongest band at 185 cm<sup>-1</sup> (514.5 nm) does not shift in going from purified to embedded in the composite SWNTs (specimen A). The frequency of RB-modes typically increase by  $\sim 7$  cm<sup>-1</sup>/GPa under hydrostatic pressure.<sup>10</sup> Therefore, within experimental resolution, one may expect residual stresses of less than 70 MPa, due to epoxy shrinkage in the curing process, provided only the hydrostatic pressure effect is taken into account. We also conclude that the bands at  $\sim 185$  cm<sup>-1</sup> (514.5 nm) stem from  $\sim 1.3$  nm diameter semiconducting nanotubes possibly of type (12,7), whereas those at  $\sim 170$  and 191 cm<sup>-1</sup> (632.8 nm) come from metallic (12,9) and (12,6) tubes, respectively.<sup>11</sup>

<sup>a)</sup>Electronic mail: vhadjiev@bayou.uh.edu

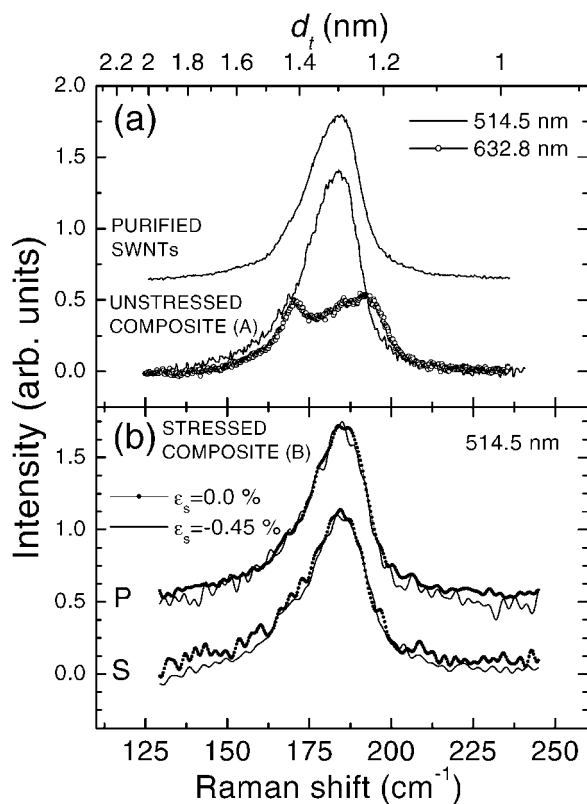


FIG. 1. Low-frequency Raman spectra of SWNTs at room temperature: (a) Spectra are measured in parallel incident and scattered light polarizations; (b) The scattering geometry is as in (a). *P* and *S* denote incident light polarizations parallel and perpendicular to the tensile stress direction, respectively. The upper horizontal scale gives the corresponding tube diameter  $d_t(\text{nm}) = 232/[\omega(\text{cm}^{-1}) - 6.5]$ .

Figure 1(b) shows the RB modes in the stressed specimen B. As seen from Figs. 1(a) and 1(b), the peak position of the RB modes remains unchanged after unloading from an *extension* tensile test for the incident light polarizations parallel (*P*) and perpendicular (*S*) to the tensile stress direction. Also, no appreciable changes are seen in Fig. 1(b) upon applying compression from zero to  $-0.45\%$  surface strain in the bending rig.

SWNTs modes shown in Fig. 2(a) involve tangential C–C bond stretching motions. Generically, they stem from the  $E_{2g_2}$  mode at  $1580\text{cm}^{-1}$  in graphite:  $E_{2g_2} \rightarrow A_{1(g)} + E_{1(g)} + E_{2(g)}$ .<sup>1</sup> Only the armchair and zig-zag SWNT modes are of even parity  $g$ . In contrast to the RB modes (Fig. 1), the graphite-like  $G$  modes in Fig. 2(a) exhibit a definite upward shift after the nanotubes were embedded in an epoxy matrix. The  $G1$  band in Fig. 2(a) is composed of  $A_{1(g)}$  and  $E_{2(g)}$  semiconducting SWNTs, whereas those in the  $G3$  band are mostly metallic.<sup>1,12</sup> Interestingly, the  $G1/G2$ -band position (specimen B) in Fig. 2(b) is different when measured for polarizations along the *P* and *S* direction. The  $G1$  frequency measured for the *S* polarization almost coincides with that of the unstressed specimen A and does not depend on the compressive strain applied in the bending rig. In contrast, the *P*-polarized  $G1$ -peak position is closer to that in purified SWNTs and shifts upward by  $3\text{cm}^{-1}$  under a compressive strain of  $\epsilon_s = -0.45\%$  along the *P* direction. A surface strain of  $\epsilon_s = -0.40\%$  pushes up the  $G1$ -peak frequency to its value in the unstressed composite. We note that

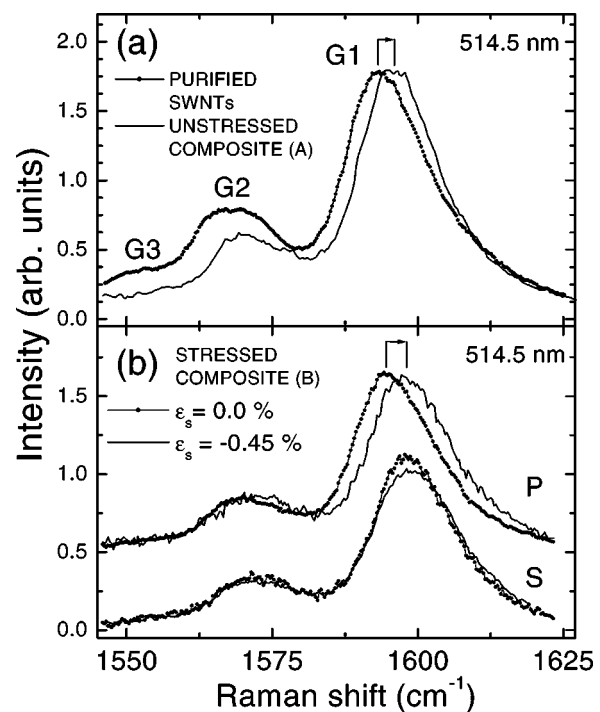


FIG. 2. High-frequency SWNTs modes measured at the same condition as in Fig. 1. The  $G1$ -peak position in (a) negligibly varies with the incident light polarization.

the Raman intensity measured in parallel polarizations is dominated by scattering from SWNTs aligned along the incident polarization direction.<sup>1</sup>

We summarize the experimental findings as follows: (i) The RB-band frequency does not change in going from purified SWNTs to composites, or upon applying compressive stresses; (ii) The  $G1$  modes exhibit an obvious upward shift after epoxy curing; (iii) A  $514.5\text{nm}$  laser line excites predominately semiconducting SWNTs; (iv) Tensile stress to failure (specimen B) releases epoxy-curing-induced strain on those SWNTs that are oriented along the applied stress direction, whereas the strain on the perpendicularly aligned nanotubes remains unchanged within experimental resolution; and (v) Composite (specimen B) compression in the bending rig to  $\epsilon_s = -0.40\%$  loads the SWNTs to the strain they have in the unstressed specimen A.

From the aforementioned findings, we conclude that the observed shift of the  $G$  modes and absence of frequency change for the RB modes excludes from consideration a van der Waals type mechanism which is found to govern the RB- and  $G$ -modes shift under hydrostatic pressure.<sup>10</sup> Rather, it suggests a direct coupling of SWNTs/ropes to the epoxy matrix. We note that although the findings (iv) may hint at the decoupling of the SWNTs as a result of the tensile stress, those in (v) evidence more for a deformation of the matrix after the tensile test that, however, preserves SWNTs–matrix coupling. Moreover, the observed  $G1$ -peak shift along with the tensile test data allows us to relate the applied stress  $\sigma_c$  on the composite to that on the embedded SWNTs. Next, we exploit this possibility in more detail.

At equilibrium, the balance of forces requires:  $\sigma_c = f\bar{\sigma}_{nr} + (1-f)\bar{\sigma}_m$ , where  $f$  denotes the nanoropes volume fraction,  $\bar{\sigma}_{nr}$  and  $\bar{\sigma}_m$  are the volume-average nanoropes and matrix stresses, respectively.  $f$  is related to the weight frac-

tion  $f_{\text{wt}}$  as  $f = f_{\text{wt}}(\rho_{\text{nr}}/\rho_m)$ . Since the nanorope density ( $\rho_{\text{nr}} \approx 1.3 \text{ g/cm}^3$ )<sup>3</sup> and that of epoxy ( $\rho_m = 1.23 \text{ g/cm}^3$ )<sup>8</sup> are very close,  $f \approx 0.01$ . We can write (Hooke's law):  $\bar{\epsilon}_c \bar{E}_c = f \bar{\epsilon}_{\text{nr}} \bar{E}_{\text{nr}} + (1-f) \bar{\epsilon}_m \bar{E}_m$ , where  $\bar{E}_c$ ,  $\bar{E}_{\text{nr}}$ , and  $\bar{E}_m$  are the elastic moduli of composite, nanoropes, and epoxy material, respectively.  $\bar{\epsilon}_c = \epsilon_s$ , (Ref. 9)  $\bar{\epsilon}_{\text{nr}}$ , and  $\bar{\epsilon}_m$  are the corresponding strains. The tensile test has given  $\bar{E}_c = 2.37 \text{ GPa}$  and  $\bar{E}_m = 2.05 \text{ GPa}$ . To a good approximation,  $\bar{\epsilon}_{\text{nr}}$  is  $\approx \epsilon_s$  due to the small value of  $f$ . This leads to  $\bar{\epsilon}_{\text{nr}} \bar{E}_{\text{nr}} = 0.153 \text{ GPa}$  for the average stress on the SWNT ropes at  $\epsilon_s = -0.45\%$ .

Unidirectional stress applied on a matrix containing a single nanorope at angle  $\phi$  to the stress direction introduces axial strain  $\epsilon_{\text{nr}}(\phi) = l_t \bar{\epsilon}_m (\cos^2 \phi - \nu_m \sin^2 \phi)$ , where  $\nu_m$  is the Poisson's ratio of the matrix. The coefficient  $l_t$  denotes transfer of the strain from the matrix to the nanorope:  $\epsilon_{\text{nr},z} = l_t \bar{\epsilon}_m$ ,  $0 \leq l_t \leq 1$ . The average nanorope strain  $\bar{\epsilon}_{\text{nr}}$  can be obtained from  $\epsilon_{\text{nr}}(\phi)$  after appropriate spacial averaging. For nanoropes that are three-dimensional (3D) randomly oriented in epoxy-resin matrix ( $\nu_m \approx 1/3$ )<sup>8</sup> averaging gives  $\bar{\epsilon}_{\text{nr}}(3\text{D}) = \epsilon_{\text{nr},z}/9$ , whereas the corresponding expression for two-dimensional (2D), random-in-plane, distribution is  $\bar{\epsilon}_{\text{nr}}(2\text{D}) = \epsilon_{\text{nr},z}/3$ .<sup>13</sup>

Next, we express the frequency change of the  $1594 \text{ cm}^{-1}$  modes with strain. Tangential vibrations of a SWNT in a nanorope remain localized on the nanotube.<sup>1</sup> Therefore, given the experimental findings (i–iv) we consider a SWNT under uniaxial stress. The corresponding axial strain  $\epsilon_z$  results in a strain  $\epsilon_{\text{ci}} = -\nu_t \epsilon_z$  along the circumference,  $\nu_t$  being the Poisson's ratio of the SWNT. The  $\epsilon_{\text{ci}}$  and  $\epsilon_z$  strains are fully symmetric in the point group of the SWNTs but not in that of the underlying graphene sheet. This results in a shear strain that also contributes to the frequency change.<sup>14</sup> We adopt the relative phonon frequency shift in the presence of strain derived in Ref. 14:  $\Delta\omega^\pm/\omega_0 = -\gamma(1-\nu_t)\epsilon_z \mp (1/2)\gamma'(1+\nu_t)\epsilon_z$ , where  $\gamma$  is the Grüneisen parameter and  $\gamma'$  the shear strain deformation potential of a SWNT. The relative shift  $\Delta\omega^\pm/\omega_0$  depends on the phonon eigenvector direction, and the splitting ( $\Delta^+ - \Delta^-$ ) is maximal for achiral SWNTs, where  $\Delta\omega^+ = \Delta\omega^{A_{1g}, E_{2g}}$  and  $\Delta\omega^- = \Delta\omega^{E_{1g}}$ . In chiral SWNTs, as those we likely probed in the Raman experiment, phonon displacements may have arbitrary directions with respect to the nanotube axis. Therefore, we observed an average shift of  $\Delta\omega(1594 \text{ cm}^{-1})/\omega_0 \approx -\gamma(1-\nu_t)\epsilon_z$ . From this expression and  $\Delta\omega(1594 \text{ cm}^{-1}) = 3 \text{ cm}^{-1}$ ,  $\gamma = 1.24$ ,<sup>14</sup> and  $\nu_t = 0.28$ ,<sup>3</sup> one readily finds  $\epsilon_z = -0.21\%$  at an external strain  $\epsilon_s = -0.45\%$  or correspondingly  $l_t = 0.5$ . Finally, from  $\bar{\epsilon}_{\text{nr}} \bar{E}_{\text{nr}} = 0.153 \text{ GPa}$ , we obtain  $\bar{E}_{\text{nr}}(3\text{D}) = 660 \text{ GPa}$  and  $\bar{E}_{\text{nr}}(2\text{D}) = 220 \text{ GPa}$ , provided  $\epsilon_{\text{nr},z} = \epsilon_z$ . The values of  $\bar{E}_{\text{nr}}$  compare well with recent results on direct tensile loading of SWNT ropes.<sup>2</sup> This comparison gives additional support to one of the important findings reported here: load is transferred predominately along the axis of the nanorope in epoxy-based composites. It also implies that SWNTs on the circumference of a nanorope in composite carry most of the load. The latter, in combination with the random distribution of the nanoropes appear to be limiting factors for efficient reinforcement of the studied composite. At the end, we estimate the strain of the nanorope due to epoxy shrinkage. The  $G$ 1-band shifts by  $\sim 2.5 \text{ cm}^{-1}$  in going

from purified SWNTs to unstressed composite [Fig. 2(a)], which translates to a compressive strain of the nanorope of  $-0.18\%$ , provided axial load transfer takes place.

Finally, we note that metallic SWNTs in the composite under stress are found to behave similarly to semiconducting nanotubes. The interpretation of the results for the metallic nanotubes, however, is more complicated and requires additional analysis beyond the scope of the present work.

In summary, we have presented an underlying methodology of a Raman scattering test. In combination with standard mechanical tests, this methodology allows the determination of residual strains due to matrix shrinkage, elastic properties of embedded in nanocomposite SWNTs/ropes, their dispersion, and load transfer effectiveness.

The authors thank Linda Schadler of Rensselaer Polytechnic Institute for sharing her experience and lending the authors the bending stage, and C. D. Scott of NASA JSC for the critical reading of the manuscript. This work was supported by the Institute for Space System Operations and Texas Center for Superconductivity at University of Houston.

<sup>1</sup>R. Saito, G. Dresselhaus, and M. S. Dresselhaus, *Physical Properties of Carbon Nanotubes* (Imperial College Press, London, 1998).

<sup>2</sup>M. F. Yu, B. S. Files, S. Arepalli, and R. S. Ruoff, *Phys. Rev. Lett.* **84**, 5552 (2000).

<sup>3</sup>J. P. Lu, *Phys. Rev. Lett.* **79**, 1297 (1997).

<sup>4</sup>J. P. Salvetat, G. A. D. Briggs, J. M. Bonard, R. R. Bacs, A. J. Kulik, T. Stöckli, N. A. Burnham, and L. Forró, *Phys. Rev. Lett.* **82**, 944 (1999).

<sup>5</sup>D. Hull and T. W. Clyne, *An Introduction to Composite Materials* (Cambridge University Press, Cambridge, UK, 1996).

<sup>6</sup>P. M. Ajayan, L. S. Schadler, S. Giannaris, and A. Rubio, *Adv. Mater.* **12**, 750 (2000); C. A. Cooper and R. J. Young, *J. Raman Spectrosc.* **30**, 929 (1999); O. Lourie and H. D. Wagner, *J. Mater. Res.* **13**, 2418 (1998).

<sup>7</sup>S. Arepalli, P. Nikolaev, W. Holmes, and C. D. Scott, *Appl. Phys. A: Mater. Sci. Process.* **70**, 125 (2000).

<sup>8</sup>Resins and Versaties Product Technical Bulletins, Shell Chemicals (P. O. Box 2465, Houston, TX 77252, Website: www.shellchemicals.com, 1998).

<sup>9</sup>The upper limit for the Raman scattering volume (RSV) in our experiment was set by the depth of focus  $\delta_f \approx 10 \mu\text{m}$  of the collecting optics used. Simple calculations for a bent beam give that the strain  $\epsilon_f$  at a depth  $\delta_f$  below the surface relates to the surface strain  $\epsilon_s$  as  $\epsilon_f = \epsilon_s + \delta_f/R$ , where  $R$  is the radius of bending. In our experiment,  $R$  of  $\approx 0.5 \text{ m}$  created  $\epsilon_s = -0.45\%$  which corresponded to  $0 \leq (\epsilon_f - \epsilon_s)/|\epsilon_s| \leq 10^{-3}$ . Therefore,  $\epsilon_s$  represents well the average strain within the RSV.

<sup>10</sup>U. D. Venkateswaram, A. M. Rao, E. Richter, M. Menon, A. Rinzler, R. E. Smalley, and P. C. Eklund, *Phys. Rev. B* **59**, 10 928 (1999).

<sup>11</sup>The RB frequency of a nanorope is found to depend on the SWNTs diameter as  $\omega(\text{cm}^{-1}) = 6.5 + 232/d_t(\text{nm})$  (see Ref. 15). On the other hand,  $d_t = d\sqrt{3(m^2 + n^2 + mn)}/\pi$ , where  $d = 0.142 \text{ nm}$  is the nearest neighbor carbon-carbon distance ( $m, n$ ) are the chiral vector components. Raman scattering from SWNTs is strongly resonant: (Refs. 1 and 12)  $514.5 \text{ nm}$  line excites mostly the semiconducting SWNTs, whereas that of  $632.8 \text{ nm}$  is more effective for excitation of the metallic nanotubes (Ref. 12). Metallic are nanotubes with  $2n + m = 3q$ , where  $q$  is an integer (Ref. 1).

<sup>12</sup>M. A. Pimenta, A. Marucci, S. A. Empedocles, M. G. Bawendi, E. B. Hanlon, A. M. Rao, P. C. Eklund, R. E. Smalley, G. Dresselhaus, and M. S. Dresselhaus, *Phys. Rev. B* **58**, 16 016 (1998); P. M. Rafailov, H. Jantoljak, and C. Thomsen, *Phys. Rev. B* **61**, 16 179 (2000).

<sup>13</sup> $\bar{\epsilon}_{\text{nr}}(3\text{D}) = \int_0^{\pi/2} \epsilon_{\text{nr}}(\phi) \sin \phi d\phi = \epsilon_{\text{nr},z}(1 - 2\nu_m)/3$ ;  $\bar{\epsilon}_{\text{nr}}(2\text{D}) = (1/\pi) \int_{-\pi/2}^{\pi/2} \epsilon_{\text{nr}}(\phi) d\phi = \epsilon_{\text{nr},z}(1 - \nu_m)/2$ .

<sup>14</sup>S. Reich, H. Jantoljak, and C. Thomsen, *Phys. Rev. B* **61**, 13 389 (2000).

<sup>15</sup>L. Alvarez, A. Righi, T. Guillard, S. Rols, E. Anglaret, D. Laplaze, and J. L. Sauvajol, *Chem. Phys. Lett.* **316**, 186 (2000).